Energy transfer and trapping in the photosystem I core antenna
A temperature study

Melanie Werst, Yiwei Jia, Laurens Mets,* and Graham R. Fleming
Department of Chemistry and the James Franck Institute, The University of Chicago, 5735 S Ellis Avenue, Chicago, Illinois 60637; and *Molecular Genetics and Cell Biology, The University of Chicago, 1101 E 57 Street, Chicago, Illinois 60637 USA

ABSTRACT The fluorescence decay kinetics of the photosystem I-only mutant strain of *Chlamydomonas reinhardtii,* A4d, are used to study energy transfer and structural organization in photosystem I (PSI). Time-resolved measurements over a wide temperature range (36–295 K) have been made both on cells containing ~65 core chl *a*/P700 and an additional 60–70 chl *a* + *b* from LHC proteins and on PSI particles containing 40–50 chl *a*/P700. In each case, the fluorescence decay kinetics is dominated by a short component, τ_1 which is largely attributed to the lifetime of the excitations in the core complex. The results are discussed in terms of simulations of the temperature dependence of τ_1 in model systems. Spectral inhomogeneity and the temperature dependence of the spectral lineshapes are included explicitly in the simulations. Various kinds of antenna arrangements are modeled with and without the inclusion of pigments with lower absorption energies than the trap (red pigments). We conclude that funnel arrangements are not consistent with our measurements. A random model that includes one or two red pigments placed close to the trap shows temperature and wavelength dependence similar to that observed experimentally. A comparison of the temperature dependence of τ_1 for cells and PSI particles is included.

INTRODUCTION

The initial steps in photosynthesis involve the transport and trapping of electronic excitations created by the absorption of light. The trapping of the excitations by a reaction center (RC) leads to efficient charge separation. The spectral and spatial arrangement of the individual pigment molecules in the antenna complex is not known in detail. A major goal of this investigation is to study energy transfer in photosystem I (PSI) and to understand the role of spectral and spatial disorder. In particular, we wish to address the question of whether or not there is some spatial arrangement, for example, a "funnel" (1) in PSI that leads to preferential migration of excitations towards the RC. Second, we wish to find out whether or not low energy antenna species (that is pigments that absorb at wavelengths longer than the trap) are used to focus excitation energy at the reaction center.

The study of energy transfer and trapping in PSI has been facilitated by detergent isolation of PSI particles containing the reaction center and various amounts of antenna complex (2–6) and by the generation of mutant strains of green algae which lack PSII (7–9). Steady-state fluorescence measurements of biochemically isolated PSI particles cannot satisfactorily be used to study energy transfer in PSI because such preparations in general contain energetically uncoupled chlorophylls which dominate the spectra because of their long lifetimes. Similarly, the steady-state fluorescence of mutants that lack PSII is dominated by the low amplitude, long lifetime component due to peripheral antenna proteins (LHCI, LHCII) not entirely deleted in the mutation. Thus, the analysis of the fluorescence decay kinetics using time-resolved spectroscopy is an essential tool for studying excitation transfer processes and structural organization in photosynthetic light harvesting systems.

The antenna complexes associated with PSI can be divided into the core and the peripheral antenna complexes. The core antenna consists of several forms of chl *a* (10) that along with the P700 RC are bound exclusively to two similar polypeptides in the 60–70 kD range (11, 12). These polypeptides also bind the initial PSI acceptors A_0, A_1 and F_x (13–15). Five additional polypeptides in the 8–20 kD range may also be found in the PSI RC/core preparations and serve as either structural components or as part of the PSI acceptor complex (13, 16, 17). The peripheral antenna complexes of PSI contain both chl *a* and chl *b* bound to several related polypeptides in the range 19–25 kD (18–20).

The core antenna complex, which is closely associated with the RC, contains only chl *a* molecules yet its spectrum is substantially broadened as compared with chl *a* in solution. This broadening indicates a distribution of site energies. Evidently, differences in the protein environment tune the spectral properties of the photosynthetic pigments. Gaussian deconvolution of absorption and emission spectra indicates at least 4–5 spectral types of chl *a* (2*b*). It has been proposed that excitations migrate preferentially from shorter to longer wavelengths towards the trap (1). Although experimental

0006-3495/92/04/868/11 $2.00

evidence in favor of such a model exists for the antenna system of certain red and blue-green algae which use a series of chemically distinct species (21), recent experiments suggest that this description may not apply to the PSI core antenna complex (2). It has also been proposed that minor low energy antenna species closely linked to the RC are necessary to focus the excitation density close to the RC (22).

Room temperature fluorescence lifetime measurements for P700-chl *a*-protein complexes isolated from barley and PSII-lacking mutants of *Chlamydomonas* revealed a linear relationship between excitation lifetime and core size (2*a*). These data were analyzed in terms of a lattice model of energy transfer in which all sites are energetically equivalent (23). From the linear dependence of the lifetime on the array size, an estimate of the single-step hopping time of 0.2 ps and the time constant for photochemical charge separation of 3 ps were obtained from the slope and intercept respectively. The variation of the spectral properties with core antenna size at room temperature showed that the energy is not concentrated in the long wavelength forms but is nearly homogenized over all the spectral forms (2). The linear relationship between lifetime and core antenna size does not extent to core plus peripheral antenna size (7). Measurements on larger PSI particles and whole cells of PSII-lacking mutants of *Chlamydomonas* showed that transfer of excitation from the peripheral to the core antenna occurs within ~5 ps (7).

To gain insight into spectral and spatial disorder in antenna systems, simulations of excitation hopping on two dimensional lattices were carried out (24). These models were chosen to mimic chl *a* pigments in the peripheral and core antenna complexes of PSI. In these models, excitation transport is assumed to occur through an incoherent mechanism, i.e., a random walk. The emission surfaces obtained from these model showed that the rising component associated with excitation transfer among different spectral forms is < 10 ps and thus these lifetimes would be very hard to detect by picosecond techniques. This study also showed that at room temperature rapid randomization or equilibration of an excitation among a representative distribution of core antenna spectral forms is a consequence of strong spectral overlap and need not be related to the spatial properties of the array. Very recently, Pullerits and Freiberg also considered spectral inhomogeneity in bacterial antenna systems (25).

The goal of the experiments reported here is to attempt to distinguish between several models of antenna organization by means of the temperature dependence of the energy transfer and trapping. The spectrally resolved temperature dependence of the trapping time is compared with model calculations. In particular, we expect different spatial arrangements of the various spectral forms that are required to reproduce the absorption spectrum to show very different temperature dependence. Low energy species, if located far from the reaction center, can act, for example, as local traps at low temperature. However, when these species are located close to the reaction center, the excitation can hop to the trap via a low energy pathway and thus these pigments can have a focussing effect.

There have been several previous studies of the temperature dependence of energy transfer in PSI (4–6, 26, 27). With the exception of the fluorescence measurements by Searle and co-workers (4) on particles containing 40 chl *a*/P700 (PSI-40), these studies have been confined to fairly large PSI particles (110–200 chl/P700) containing peripheral as well as core antenna. The study of Searle and co-workers was carried out with an instrument function of 300–400 ps (4). This relatively poor time resolution may not be adequate to obtain the temperature dependence accurately.

Low temperature (77 K) fluorescence decay kinetics of larger PSI particles have been studied by Wittmershaus (110 chl/P700) and Mukerji and Sauer (200 chl/P700). At low temperature a fast decay is observed for emission wavelength of ~680 nm and a rise time at emission wavelength 735 nm (5, 6). This was interpreted as energy transfer between different antenna pools. Wittmershaus (5) proposed that the red pigments are organized in the "internal" and peripheral antenna, and are responsible for the 710–735 nm fluorescence at low temperature. These red pigments are linked to the core antenna and act as intermediate traps for excitations transferred to P700 (5). Mukerji and Sauer (6) proposed that the red pigments are present in the peripheral antenna in agreement with their observation that isolated LHCI shows red fluorescence at low temperature (28). However, the function of these red pigments in the peripheral antenna is not clear. Mukerji and Sauer proposed that these pigments facilitate energy transfer to the reaction center or possibly act as a photoprotection devices for the reaction center (28).

To model the temperature dependence of energy transfer in PSI, Gillie et al. (27) used multiphonon radiationless transition theory and concluded that the single-step transfer rate decreased strongly at low temperatures, in accord with their hole burning data on PSI-200 particles at 1.6 K. The experiments suggest a time scale for energy transer of ~300 ps at this temperature, enormously slower than the estimate of 200 fs by Owens et al. (2*a*) at room temperature. In contrast, recent measurements by van der Laan et al. (29) show that the energy transfer time from B800 to B850 in *Rhodobacter sphaeroides* is ~2 ps in the range 1.2–30 K. A calculation based on pump-probe experiments has

been reported recently by Lyle and Struve (26) which yields a transfer time several times longer than that reported by Gillie et al. (27). Both of these studies (26, 27) model an individual energy transfer step rather than the overall trapping dynamics in an inhomogeneous antenna. As described above we wish to consider the antenna inhomogeneity explicitly and, thus, a different approach is required.

The availability of a very detailed set of Franck-Condon factors for PSI from the work of Small and co-workers (27) provides us with the opportunity to model the absorption spectrum of the PSI core antenna directly. The approach has been described in detail in a separate publication (30). In outline, we use a room temperature Gaussian deconvolution procedure (30) to determine the number of spectral types required to model the absorption spectrum. The absorption spectrum of each type is calculated fully quantum mechanically (31) for 42 modes, including a low frequency phonon mode. In this approach if all relevant degrees of freedom are included, dephasing is self consistently described (32) and the temperature dependence of the spectral width can be calculated directly. Once the temperature dependent spectra are known, rather than estimate coupling parameters, Förster theory can be used directly to calculate the elementary energy transfer rates. These parameters can then be fed directly into a master equation model (24) of any particular spatial or spectral model.

The present investigation concerns the temperature dependence of the time-resolved fluorescence decay of whole cells of the PSI-only mutant strain of *Chlamydomonas,* A4d and PSI core particles isolated from this strain. A4d lacks PSII and 95% of the LHCII proteins (7). In addition, A4d has a reduced core antenna size (60–65 chl *a*/P700) relative to that of wild type cells (120 chl *a*/P700) and a slightly altered LHCI composition (7). The LHC proteins in A4d contribute 60–70 chl $a + b$ per RC. PSI particles isolated from A4d cells contain 40–50 chl *a*/P700. Decay measurements are made over the range 36–295 K.

MATERIALS AND METHODS

C. reinhardtii strain A4d was grown in low light on Tris-acetate-phosphate (TAP) medium (33). For analysis of the fluorescence from whole cells, the culture was harvested by centrifugation and the cells were resuspended in fresh TAP medium containing 60% glycerol. PSI particles were purified from the same strain by polyacrylamide gel electrophoresis of octyl-glucoside solubilized membranes. Cultures were grown in TAP medium to a density of $\sim 5 \times 10^6$ cells/ml, harvested by centifugation and resuspended at a concentration of 3×10^9 cells/ml in ice cold buffer A (50 mM Tris-Cl, pH 7.0, 10 mM NaCl, 5 mM MgCl, 5 mM amino-caproic acid, 1 mM benzamidine HCl). This suspension was passed twice through a prechilled French pressure cell at 4,000 psi and cell debris removed by centrifugation at 500 *g* for 1 min. The membranes were then pelleted by centrifugation at 5,000 *g* for 10 min. The membrane pellet was washed twice by resuspension in buffer A and recentrifugation under the same conditions. The final pellet was resuspended in buffer A containing 10% glycerol at a concentration of 0.35 mg chl/ml and stored in aliquots at −80°C. For solubilization, membranes containing 1.0 mg chl were pelleted by centrifugation, resuspended in ice cold electrophoresis buffer (12.4 mM Tris, 48 mM glycine), repelleted and resuspended in 0.3 ml of the same buffer. 0.5 ml of 10% octyl glucoside in water was added and the mixture incubated on ice for 30 min. Insoluble material was removed by centrifugation at 10,000 *g* for 10 min. To the supernatant was added 78 μl of 50% sucrose and 48 μl 10% Deriphat 160 detergent. After 10 min on ice, the sample was loaded on a preparative electrophoresis gel and run essentially as described by Peter et al. (34) with minor modifications for preparative conditions. 10% acrylamide (100:1 acrylamide:Bis-acrylamide) gels were 4.9 mm thick, 13.8 cm wide, 13.5 cm long and buffered with 12.4 mM Tris, 48 mM glycine containing 0.1% Deriphat 160. The upper electrode buffer also contained 0.1% Deriphat 160, but detergent was omitted from the lower electrode solution. Electrophoresis was performed in a cold room at 3.5 mA, 25 V for 16 h. The dark green, nonfluorescent PSI band was excised from the gel, sealed in a dialysis bag, and slowly equilibrated in 60% glycerol by dialysis for ~6 h. The resulting sample formed a clear glass at low temperature and showed the same room temperature fluorescence decay kinetics as samples not treated with glycerol.

Chl *a*/P700 ratios were determined on PSI particles eluted from the electrophoresis gel before addition of glycerol. The gel was macerated by squeezing twice through a hole made in the bottom of a 1.5-ml microcentrifuge tube with a 27 gauge needle. The gel pieces were suspended in an equal volume of ice-cold distilled water and held over night. The clarified supernatant was used to measure light-induced absorbance changes at 697 nm for the estimation of P700 (10) using a differential extinction coefficient of 64 mM^{-1} cm^{-1} (35). Chl *a* content was estimated using an extinction coefficient of 60 mM cm^{-1} at 677 nm (36). Chl *a*/P700 ratios ranged from 40–50 (consistent, within experimental error) for these PSI particle preparations. Fluorescence measurements were recorded using a Spex 112 spectrofluorometer. Emission spectra were corrected for variations in source intensity and detector sensitivity.

Fluorescence decay measurements were performed using time-correlated single photon counting as described previously (2, 7, 37). Samples were cooled using a closed circuit helium refrigerator and front surface fluorescence was collected and detected by a 6-μm microchannel plate PMT (Hamamatsu R2809U-01). The instrument response was measured from the scattering of excitation light by the sample, either whole cells or PSI-particles and had a FWHM of 50–60 ps. The samples were excited at 650 nm and the emission was monitored at wavelengths 680, 690, 700, 710, and 720 nm.

The measured fluorescence decays were fit to a weighted sum of exponential decays through iterative convolution with the instrument response function as described previously (2, 7, 37). The fluorescence decay impulse response was described by

$$F(t) = \Sigma A_i e_i^{-t/\tau} \text{ with } \Sigma A_i = 1.0,$$

where τ_i is the lifetime of each individual component and A_i is the corresponding preexponential amplitude. The quality of the fits was judged by a reduced χ^2 criterion, a runs test and a plot of the weighted residuals. The fluorescence decay of oxazine 725 (Exciton) in methanol was used as a standard. The pulse intensity is 5×10^{11} photons cm^{-2} $pulse^{-1}$. Reduction in the excitation intensity by a factor of 20 did not alter the fluorescence decay kinetics indicating that excitation annihilation processes did not contribute to the observed decays.

RESULTS

Time-resolved fluorescence analysis of whole cells

The fluorescence decay of intact cells of the PSI-only mutant A4d suspended in 60% glycerol monitored at emission wavelengths 680, 690, 700, 710, and 720 nm over the temperature range 36–295 K is accurately described ($\chi^2 < 1.15$) by four exponential decay components. Fig. 1 shows typical fluorescence decay data. For all the wavelengths monitored except 720 nm at temperatures < 160 K, the four lifetimes are in the range 20–60 ps (50–70%), 150–350 ps (20–30%), 500–1,200 ps (10–15%) and 2,000–5,000 ps (3–8%). The lifetimes for the decays monitored at 720 nm at temperatures < 160 K are in the range 70–120 ps (30–50%), 300–400 ps (30–40%), 1,000–1,500 (10–20%) and 2,000–4,000 ps (6–10%).

The short component (τ_1) dominates the fluorescence decay. Owens et al. (*2a*) previously showed that P700 activity is directly correlated with the amplitude of the short component. This short component is largely due to the lifetime of the excitations in the core complex with some small contribution due to energy transfer from the peripheral to the core complex. Energy transfer from the peripheral to core antenna in A4d cells has been estimated to be <5 ps at room temperature (7). The intermediate lifetime (200–400 ps) has spectral characteristics of both the peripheral and core antenna pigments (*2b*). Lifetimes in this range are typically associated with chl *b* and peripheral antenna complexes. Because of the absence of intermediate lifetime components in RC/core antenna preparations lacking chl *b*, it has been proposed that the 150–450 ps components originate as the result of interactions between peripheral and core antenna pigments which induce the formation of minor pigment aggregates in the core antenna (*2b*). The long components (τ_3, 500–1,500 ps, τ_4, 2,000–4,000 ps), are attributed to peripheral antenna complexes lacking a trap and to uncoupled chlorophylls. Decay components in the range of 750–2,400 ps have been found in monomeric and oligomeric forms of LHC in vitro and in a *C. reinhardtii* strain, C2, which lacks both PSI and PSII (38). The longer components observed here are probably due to the remaining LHC proteins and any energetically disconnected chlorophyll in the cells. Rising components (negative preexponential amplitudes) were not observed for any of the lifetimes in the decays even though such terms were routinely included in the range of the initial estimates used for each regression analysis.

The room temperature fluorescence decay of A4d cells (excitation at 650 nm, emission monitored at 690 nm) suspended in water (as opposed to 60% glycerol) is accurately described by three exponential components with lifetimes in the range 40 ps, 350 ps, and 1,400 ps (Table 1). It appears that suspending the cells in 60% glycerol, necessary for obtaining a glass at low temperature, perturbs the cells such that a fourth long compo-

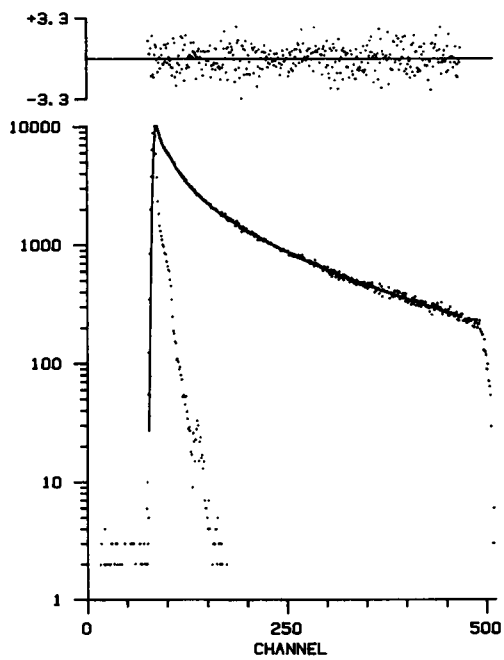

FIGURE 1 Fluorescence decay of A4d cells suspended in 60% glycerol. The measured decay is fit to a weighted sum of exponential decays [$F(t)$] through iterative convolution with the instrument function.

$$F(t) = 0.590 \exp(-t/28.3 \text{ ps}) + 0.223 \exp(-t/153.7 \text{ ps}) + 0.129 \exp(-t/594.7 \text{ ps}) + 0.060 \exp(-t/2146.7 \text{ ps}).$$

Shown above are the normalized residuals for the fit from the least squares regression. Excitation wavelength = 650 nm, emission collected at 690 nm. Temperature = 36 K, 9.8 ps/channel, $\chi^2 = 1.02$.

TABLE 1 **Comparison of time-resolved fluorescence of A4d cells in (*A*) water, and (*B*) 60% glycerol**

		Component 1	Component 2	Component 3	Component 4
(*A*)	$\tau_i(A_i)$	40 ps (60%)	350 ps (25%)	1,200 ps (15%)	—
	yield	8%	30%	62%	
(*B*)	$\tau_i(A_i)$	40 ps (60%)	300 ps (20%)	1,400 ps (9%)	4,000 ps (9%)
	yield	4%	11%	22%	63%

The yields (%) for the individual decay components, that is the contribution of the individual components to the total steady-state fluorescence, are also shown. Excitation wavelength = 650 nm, emission wavelength 690 nm, T = 295 K.

nent of 2–4 ns is required to fit the decay (Table 1). The addition of glycerol to whole cells does not appear to strip core chlorophyll from the PSI core antenna and RC. This would result in a decrease in lifetime of τ_1 (*2a*). Nor does it appear to be uncoupling core antenna complexes from a functional trap. This is expected to cause a decrease in the amplitude of component 1 with a corresponding increase in the long component (*2a*). It does cause a reduction in the amplitude of components 2 (300–400 ps) and 3 (1,200–1,500 ps) which are associated with the peripheral antenna proteins and a corresponding emergence of a long lifetime, fourth (2–4 ns) component. The origin of this long fourth component is not clear. It might be due to LHC protein aggregates or to free chlorophyll. The lifetime of free chl in solution is 5 ns (39).

The lifetime of the short decay component in A4d cells is relatively independent of temperature in the range 36–295 K for emission wavelengths 680, 690, 700, and 710 nm (Fig. 2). Linear regression of the data shows the lifetime of the short component monitored at 680 nm

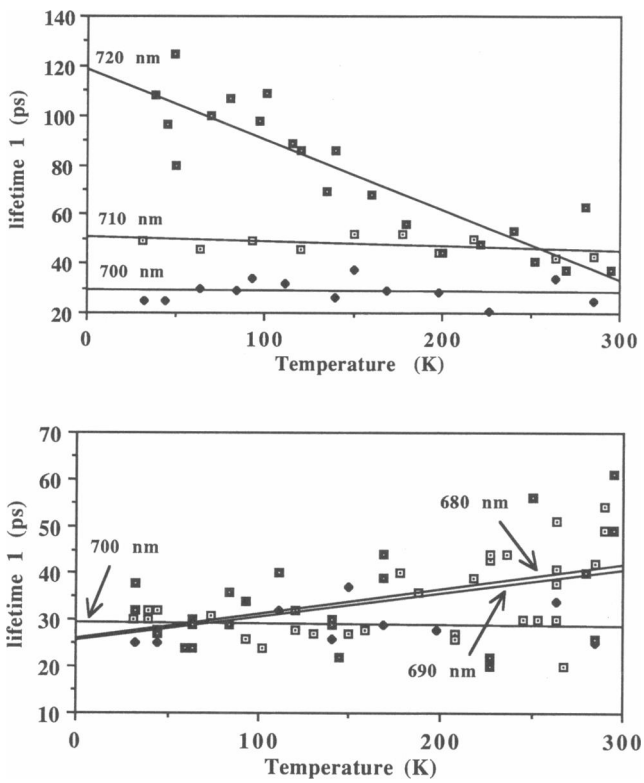

FIGURE 2 Temperature dependence for τ_1 for A4d cells at emission wavelengths 680, 690, 700, 710, and 720 nm. The excitation wavelength is 650 nm. The top panel shows wavelengths 700 nm (*diamonds*), 710 nm (*open squares*), and 720 nm (*solid squares*). The bottom panel shows wavelengths 680 nm (*solid squares*), 690 nm (*open squares*) and 700 nm (*diamonds*).

and 690 nm decreased slightly from ~45 ps at 295 K to 25 ps at 36 K (Fig. 2, *bottom*). The fast component monitored at 700 nm shows negligible change over the temperature range 36–295 K. The lifetime monitored at 710 nm increased very slightly as the temperature decreases from 295 to 36 K whereas the lifetime monitored at 720 nm increased considerably from 40 ps at 295 K to 110 ps at ~36 K (Fig. 2, *top*). At room temperature, τ_1 is relatively independent of emission wavelength (45 ± 15 ps). The longer lifetimes at 710 and 720 nm in comparison to 680, 690, and 700-nm emission and the considerable increase in the 720-nm lifetime as the temperature is cooled from 295 to 36 K most likely reflect activated energy transfer to the trap from pigments whose relaxed excited state lies below the trap. The decrease in the lifetime of the short component when monitored at 680 and 690 nm indicates that the endothermic detrapping rate is slowed relative to the trapping rate as the temperature is lowered with the net effect of increasing the overall trapping rate.

The amplitude of the short component for emission wavelengths 680, 690, 700, and 710 nm is essentially constant in the range 36–295 K. The amplitude for the short component monitored at 720-nm emission is slightly smaller (30–60%) than the amplitude for emission at 680, 690, 700, and 710 nm (50–70%). The amplitude of the short component monitored at 720 nm decreases from 60% at 295 K to 30% at 36 K.

The lifetime and amplitude of the intermediate and long lifetime components τ_2: 150–300 ps, τ_3: 600–1,200 ps, τ_4: 2,000–4,000 ps also show very little change as the temperature is lowered from 295 to 36 K for all emission wavelengths except 720 nm. At 720 nm, there is an increase in τ_2 and τ_3 from 100–200 ps and 400–600 ps respectively at temperatures in the range 160–300 K to 300–500 ps and 1,000–1,800 ps at temperatures < 140 K. Thus, the yield at 720 nm from these intermediate and long components increases considerably as the temperature is lowered.

Steady-state fluorescence of A4d cells

Steady-state fluorescence spectra of A4d cells suspended in glycerol have been measured at room temperature and 77 K. At room temperature, the maximum intensity is at 680 nm, with a broad low intensity shoulder in the range 700–750 nm. The 77 K emission spectrum shows the 680 nm fluorescence band seen at room temperature and increased intensity in the range 700–750 nm with maximum intensity at 712–720 nm. The intensity of the red fluorescence in the range 700–750 nm relative to that at 680 nm is somewhat variable,

differing for different batches of cells and the rate at which cells are cooled.

It has been shown that room temperature steady-state emission of A4d cells in the absence of glycerol (7) is largely derived from pigments that contribute to the slow decay component even though this slow component accounts for only a small percent of the total time resolved amplitude. The contribution of the short lifetime component (40–50 ps) to the total room temperature steady-state fluorescence (i.e., the yield) at 690 nm is calculated to be ~8% (Table 1). The long lifetime, characteristic of uncoupled LHC proteins (1,200–1,500 ps) in A4d cells, accounts for >60% of the room temperature yield at 690 nm (Table 1). In the case of cells suspended in 60% glycerol (Table 1) the short component accounts for an even smaller percent of the yield (<5%) at 690 nm. The long components τ_3, τ_4 (1–5 ns) account for ~90% of the room temperature yield at 690 nm. Similarly, the room temperature and 77 K emission at other wavelengths (680–720 nm) is dominated by the long decay components and does not reflect energy transfer in the core antenna and RC.

We note that the lifetimes τ_2 and τ_3 monitored at 720 nm increased significantly as the temperature is lowered below 160 K. This could account for the increase in the steady-state fluorescence in the range 710–750 nm at 77 K. These two lifetimes are related to the peripheral light harvesting proteins in A4d cells. It is possible that at low temperature LHCI becomes disconnected from the core and RC and can no longer transfer energy to the trap. This results in an increase in fluorescence from LHCI. Alternatively, there may be aggregation effects at low temperature that result in increased fluorescence at long wavelengths (40).

Time-resolved fluorescence analysis of PSI particles

The fluorescence decay of PSI-40 particles obtained from A4d cells over the temperature range 36–295 K is accurately described ($\chi^2 < 1.15$) by four exponential components. For emission at wavelengths 680 and 690 nm, the lifetimes are in the range 10–25 ps, 40–300 ps, 300–1,200 ps and 3,000–6,000 ps. The short component (10–25 ps) dominates the decay (80–90%) and represents the decay of the excitations in the core antenna of PSI whose lifetime is limited by the efficient photochemical quenching on P700. For wavelengths 700, 710, and 720 nm the short decay is in the range 15–50 ps (70–90%), 20–80 ps (40–80%), and 20–95 ps (40–80%), respectively. The intermediate decay, τ_2 is attributed to a small amount of particles with a core of 45–65 chl *a*/P700 and with connected peripheral antenna proteins. Lifetimes in the range 500–1,200 ps are associated with disconnected LHC proteins in these preparations. The long fourth component is attributed to either free chlorophyll or LHC aggregates. No rising components are observed (negative preexponential amplitudes) even though such terms are routinely searched for in the fits. Fig. 3 shows typical fluorescence decay data for PSI particles; the decay shown is monitored at 680 nm at 50 K.

PSI gels obtained from polyacrylamide gel electrophoresis were slowly equilibrated in 60% glycerol by placing them in dialysis tubing in a bath of 60% glycerol in the cold as described in Methods. This procedure for obtaining glassy sample at low temperature resulted in material whose room temperature kinetics is unchanged with respect to material not treated with glycerol (Table 2) and this procedure was used for all low temperature studies. Attempts to run gels in acrylamide in 60% glycerol were unsuccessful. Such preparations resulted in large amounts of free chlorophyll. Placing the gel pieces directly in 60% glycerol also resulted in altered kinetics (Table 2). The amplitude of the fast component,

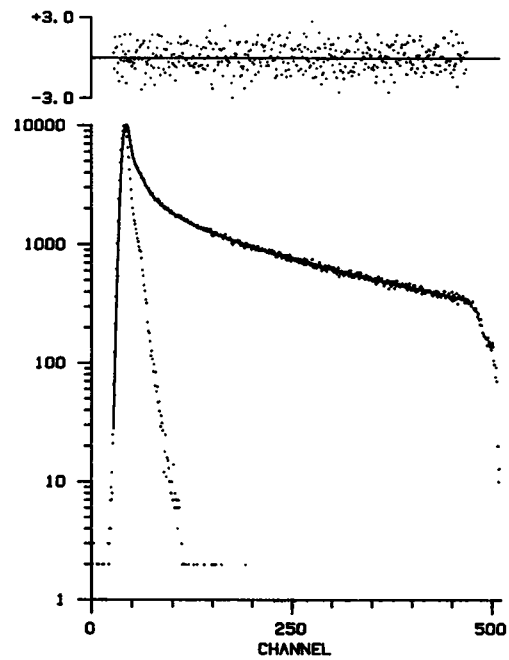

FIGURE 3 Fluorescence decay of PSI particles isolated from A4d. The measured decay is fit to a weighted sum of exponential decays [$F(t)$] through iterative convolution with the instrument function.

$$F(t) = 0.910\exp(-t/12.4\text{ ps}) + 0.045\exp(-t/122.7\text{ ps}) + 0.026\exp(-t/532.4\text{ ps}) + 0.024\exp(-t/2525.2\text{ ps}).$$

Shown above are the normalized residuals for the fit from the least-squares regression. Excitation wavelength 650 nm, emission collected at 690 nm. Temperature = 50 K, 8.3 ps/channel. $\chi^2 = 0.97$.

TABLE 2 **Time resolved fluorescence for A4d PSI gel containing 40–50 chl *a*/P700**

		Component 1	Component 2	Component 3	Component 4
(*A*)	$\tau_i(A_i)$	17 ps (87%)	103 ps (7%)	1,000 ps (3%)	4,364 ps (4%)
	yield	6%	4%	13%	77%
(*B*)	$\tau_i(A_i)$	17 ps (84%)	85 ps (10%)	800 ps (2%)	4,414 ps (4%)
	yield	7%	4%	7%	82%
(*C*)	$\tau_i(A_i)$	29 ps (44%)	95 ps (42%)	360 ps (11%)	3,000 ps (8%)
	yield	3%	13%	12%	72%

(*A*) gel without glycerol, (*B*) gel slowly equilibrated in 60% glycerol, (*C*) gel directly added to 60% glycerol. The contribution of the individual decay components to the total steady-state fluorescence (yield) are also shown. Excitation wavelength = 650 nm, emission wavelength = 690 nm, Temperature = 295 K.

indicative of the presence of efficient quenchers of excitation energy was considerably reduced (87–44%) when gel pieces were placed directly in 60% glycerol. There is also a corresponding increase in the amplitude of the longer components. Reduced P700 activity is directly correlated with a reduction in the amplitude of the short component (2*a*).

Fig. 4 shows the dependence of the lifetime of the short component on temperature for PSI particles isolated from A4d. Linear regression shows the short lifetime monitored at 690 decreases slightly as the temperature is lowered from 295 to 36 K. The lifetime of PSI particles monitored at 680 nm shows negligible temperature dependence in this range. For wavelengths 700, 710, and 720 nm, the lifetime of the short component increases from ~20 ps at 295 K to 50, 80, and 90 ps, respectively, at 36 K. At room temperature τ_1 is independent of emission wavelength. The lifetimes of components 2, 3, and 4 at wavelengths 680–720 nm showed negligible temperature dependence in the range 36–295 K. We note that the 720 nm emission for cells showed considerable increases in τ_2 and τ_3 at temperatures <160 K in contrast to the results for PSI particles. This is consistent with the assignment of these components to peripheral light harvesting proteins which are considerably reduced in these PSI preparations.

The shorter lifetime observed at 690 nm for the PSI particles (40–50 chl *a*/P700) in comparison to A4d cells (60–70 chl *a*/P700, plus ~60 chl *a* + *b* in LHC) is shown in Fig. 5 and reflects the smaller PSI antenna size resulting from the isolation procedure. At room temperature, the lifetime τ_1 of A4d cells is ~40 ps whereas the lifetime of PSI particles is ~18 ps. Based on the linear dependence of lifetime on core size (2*a*), an increase of ~20 chl *a* in the core antenna could account for most of this increase. The transfer from the peripheral to core antenna has previously been estimated to be <5 ps (7). For both cells and particles, the lifetime of the short component monitored at 690 nm decreases with temperature and reflects slowed detrapping relative to trapping, resulting in a small increase in the overall trapping rate. The trend in the temperature dependence of the short component for cells and particles is similar (Fig. 5), indicating that the excitation dynamics monitored at 690 nm is essentially the same for both particles containing a core of 40–50 chl *a* and cells containing a 65 chl *a*/P700 core plus an additional 60 peripheral antenna chlorophyll (chl *a* + *b*). The decrease in τ_1 with decreasing temperature is greater for cells than PSI particles. This might be due to an increase in the energy transfer rate from the peripheral to core antenna as the temperature decreases and would suggest that the peripheral antenna pigments are relatively "bluer" than those of the core complex.

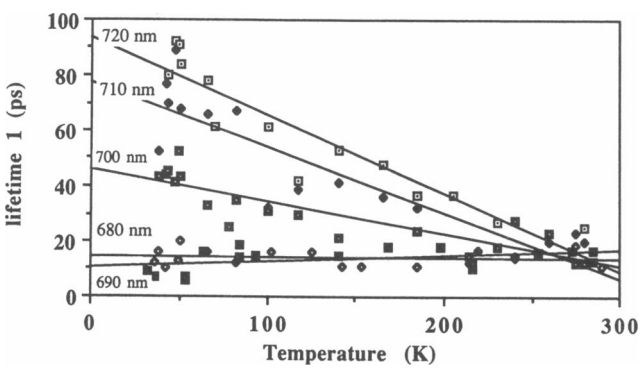

FIGURE 4 Temperature dependence of τ_1 for PSI particles isolated from A4d. Emission wavelengths are 680 nm (*open diamonds*), 690 nm (*solid squares*), 700 nm (*solid square with open center*), 710 nm (*solid diamonds*), and 720 nm (*open squares*). The excitation wavelength is 650 nm.

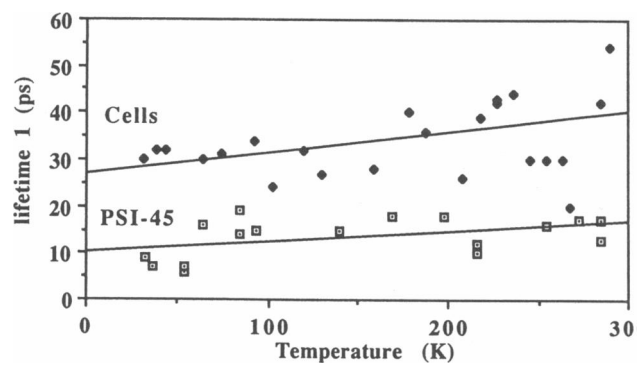

FIGURE 5 Temperature dependence of τ_1 for A4d cells (*diamonds*) and A4d PSI particles (*squares*). The excitation and emission wavelength is 650 nm and 690 nm, respectively.

Steady-state measurements of PSI particles

The room temperature steady-state fluorescence of PSI-40 gel pieces slowly equilibrated in glycerol shows a band at 680 nm with a low intensity shoulder in the range 700–750 nm. Upon cooling, the spectrum narrows, however, there is no red shift of the emission maximum from ~680 nm and no significant increase in the intensity of the emission in the range 700–750 nm. Analysis of the yields due to the four decay components (Table 2) of PSI particle shows that the short component accounts for <8% of the yield at 690 nm. The contribution of the short decay to the overall steady-state fluorescence at room temperature and low temperature is also minor at other wavelengths in the range 680–720 nm. Thus, the steady-state fluorescence emission is almost entirely dominated by the relatively small amounts of long decay component due to disconnected chlorophyll and does not reflect the fluorescence from the core antenna and RC.

Samples which are slowly equilibrated in glycerol have a short lifetime that dominates the kinetics at 690 nm and thus contain efficient quenchers of excitation energy. We therefore conclude that these samples contain a functional trap. It has been argued from biochemical studies that the 680–690 nm emission reported for PSI-40 particles from algae and higher plants is an artefact of chl-surfactant interaction and that the true fluorescence from PSI core and RC at 77 K is at 715 nm (41). We regard this as highly unlikely because the observed short lifetime that dominates the decay at 690 nm (80–90%) would not be expected if this emission were due to partly detached chlorophyll. It has been shown previously that P700 activity is directly correlated with the amplitude of the short component (2*a*). PSI preparations have been reported which show different low temperature steady state fluorescence (42–45). However, we need to emphasize that the steady-state fluorescence emission of these preparations reflects the long lifetime components (1–5 ns) that account for >80% of the yield at any given wavelength and which are not related to energy transfer in the core and RC.

DISCUSSION

Simulations

To interpret the temperature and spectral dependence of the trapping time, we have made preliminary attempts to reproduce this temperature and wavelength dependence in model systems. The theoretical basis for these simulations has been described in detail in a separate publication (30). Our approach to energy transfer in PSI is based on a Förster hopping model. Both the Förster rate and energy trapping kinetics are temperature dependent. The former relationship arises through the temperature dependence of the spectral overlaps and the latter from the detailed balance prescription relating forward and reverse rates:

$$k_{ij} = k_{ji} x \exp[-\delta A_{ij}/kT],$$

where δA_{ij} is the difference between the peak frequencies of the two absorption (or emission bands). This insures that in the absence of trapping the site populations relax to a Boltzmann distribution at each temperature.

Simulations of energy transfer were performed using an array of 49 pigments: 48 core antenna and one RC pigment. The number of sites in the model approximates the core antenna size in the experimental PSI preparations. The spectral properties of the models were chosen to mimic the chl *a* spectral distribution in the PSI core complex. The number of pigments of each spectral type as well as their absorption and emission maxima are given in reference 30. The following models were simulated. The first is the funnel model in which the core antenna types are arranged so that the absorption spectra of the individual pigments shift progressively to longer wavelengths as the distance from the trap decreases. A random model is also generated in which the pigments are haphazardly arranged around the trap and the decays are averaged over 50 configurations. Additional models are generated that include one or two red pigments that absorb at a wavelength redder than the trap (702–705 nm). In the funnel model with red pigments, the red pigments are placed either close to or away from the trap. In the random model with red pigments, these red pigments are either randomly arranged over 50 configurations or placed close to the trap.

The calculations begin with a fully quantum mechanical calculation of the temperature-dependent spectra of the various spectral types, using the Hamiltonian of Harris et al. (32) and the Franck-Condon factors of Small and co-workers (27). Following this the appropriate master equations are solved as described by Jean et al. (24).

Simulations of the funnel model without red pigments show that the lifetime of the excitations in the core decreased from 24 ps at 298 K to 4 ps at 77 K and is independent of emission wavelength. This result is expected because at low temperature (77 K), the excitation is concentrated on the RC in less than a few picoseconds and the energy transfer from the RC back to the core antenna (back transfer) is slow due to the Boltzmann factor. Thus, the overall trapping time is limited by the charge separation rate. These simulations

suggest that the small temperature effects observed experimentally are not consistent with a funnel description of antenna organization and energy transfer. Such an arrangement would result in a considerable decrease in the lifetime of the excitations in the core at low temperature. This model can clearly be excluded based on our experimental results.

Simulations using the funnel model with two red pigments close to the trap show very weak temperature dependence, with τ = 35 ps at 298 K and 41 ps at 77 K for wavelengths in the range 680–720 ps. There is no emission wavelength dependence in this model. This results from the spectral arrangement in which each spectral type has a similar group of surrounding pigments. The temperature dependence can be explained by the balance of the rapid concentration of excitations on the red pigments and the slow transfer from the red pigments to the reaction center. The lack of spectral dependence enables us to exclude this model. We observe that the lifetime increases considerably with decreasing temperature for wavelengths 680–690 nm for any funnel model with red pigments not close to the reaction center (30). Again, this is not consistent with our experimental results.

The lifetime of the excitations at 298 K for the random model which includes two red pigments is ~50 ps and shows negligible wavelength dependence. At 77 K, the decay kinetics is multiexponential and strongly wavelength dependent, a 9-ps decay time is observed at 680 nm whereas a 15-ps risetime is observed at 720 nm (30). This wavelength dependence is considerably greater than that observed experimentally. The multiexponential kinetics can be explained by the existence of "alternative traps," that is, the red pigments that are surrounded by bluer pigments and a "local funnel pathway" in an overall random model. This extreme wavelength dependence is not observed in our experiments and thus, a random arrangement with two or more red pigments seems highly unlikely. However, we note that the moderate wavelength dependence observed for the random model with 1 red pigment (30) is not sufficient to rule out this model.

The lifetime of the excitations in the core for a random model without red pigments at room temperature is ~36 ps and emission wavelength independent. Because the simulated decays at low temperature are quite complex, to compare with experiment we added two small-amplitude long lifetime components (800 ps and 4 ns) and convoluted the simulated curve with a measured instrument response function. We previously showed (24) that even small amounts of long components can severely compromise the ability to detect short components or multi-exponentiality in real data. On fitting the resulting curve and extracting the short component we find that at 77 K, the lifetime increases from 13 to 21 ps for emission wavelengths in the range 680–700 nm. The lifetime decreases from 21 ps to 14 ps for emission wavelength from 700 nm to 720 nm. This behavior is not consistent with our experiments.

We conclude from the simulations of the funnel model with red pigments that there must be spectral inhomogeneity to observe a wavelength dependence of the decay time. In addition, the funnel model with the red pigments not close to the trap shows a very strong temperature dependence for wavelengths 680 and 690 nm (30). The strong wavelength dependence observed for the random model with the two red pigments randomly placed in the array also allows us to exclude the model. We note that the wavelength dependence observed for the random model with 1 red pigment is not sufficient for us to rule out this model. We have also carried out a simulation using a random model in which the red pigments are placed close to the trap. At 298 K, this model gives a lifetime of 41 ps with little wavelength dependence. At 77 K, we added long components and convoluted as described above. Now the short component varies from 10 ps to 57 ps as the emission wavelength increases from 680 to 720 nm. Thus, this model shows the same trends in the wavelength and temperature dependence as the experimental data. The 77 K steady-state fluorescence calculated for this two dimensional array of 49 sites shows fluorescence emission at 700–750 nm that is considerably more intense than the emission at 680 nm. The steady-state fluorescence observed experimentally does not show strong red fluorescence at 77 K but this is because the observed fluorescence is dominated by relatively small amounts of long lifetime (1–5 ns) components.

We note that an increase in the lifetime τ_1 with decreasing temperature is observed at wavelengths $\geq$ 710 nm for cells and $\geq$ 700 nm for PSI particles (Figs. 2 and 4, respectively). When the emission wavelength is increased from 700 to 720 nm, the contribution of the fluorescence emission from the long wavelength pigments with core increases. It is these long wavelength pigments that are responsible for the increase in the fluorescence lifetime τ_1. The different temperature dependence of τ_1 in the 700-nm region of cells and PSI particles can be explained if we assume that the percentage of red pigments in the cells is less than in particles, and thus, the contribution of fluorescence from red pigments in cells is less than in particles at 700 nm. We would, therefore, expect that the increase of τ_1 with temperature occurs for cells at longer wavelengths than for particles. This argument leads to the conclusion that the peripheral antenna present in A4d cells is composed of spectral types that are relatively bluer than those of the core and RC.

CONCLUDING REMARKS

The only simple lattice model that is consistent both with the absorption spectra and the wavelength and temperature dependent lifetime data for PSI particles is a random model which includes one or two low-energy pigments; if two red pigments are included, these must be placed close to the reaction center. The location of low energy antenna species close to the trap was proposed by van Grondelle and co-workers for bacterial antenna systems (46, 47). The rationale for such an arrangement is that excitations spend more time in the vicinity of the trap and this enhances the probability of initiating charge separation. At room temperature, equilibration among all spectral types is reached in <5 ps. After equilibration is reached, the low energy pigments have twice as high a probability of being in the excited state. When these pigments are close to the RC, the excitation can hop to the trap via a low energy pathway. Thus, even at room temperature, these red pigments placed close to the RC have a focussing effect. Our results are not consistent with a funnel model for antenna organization, whether or not red pigments are placed in the array. Finally, comparison of the dependence of τ_1 with temperature for cells and PSI particles suggests that the spectral types of the peripheral antenna are bluer than those of the core complex.

The authors would like to thank Aida Pascual for her help in preparing samples.

This work was supported by a grant from the National Science Foundation. Melanie Werst was the recipient of a postdoctoral fellowship from the Center for Photochemistry and Photobiology at the University of Chicago and from the National Institutes of Health (GM 14458-01).

Received for publication 15 July 1991 and in final form 19 November 1991.

REFERENCES

1. Seeley, G. R. 1973. Energy transfer in a model of the photosynthetic unit of green plants. *J. Theor. Biol.* 40:189–199.
2*a*. Owens, T. G., S. P. Webb, L. Mets, R. S. Alberte, and G. R. Fleming. 1987. Antenna size dependence of the fluorescence decay in the core antenna of photosystem I: estimates of charge separation and energy transfer rates. *Proc. Natl. Acad. Sci. USA.* 84:1532–1536.
2*b*. Owens, T. G., S. P. Webb, R. S. Alberte, L. Mets, and G. R. Fleming. 1988. Antenna structure and excitation dynamics in photosystem I. I. Studies of detergent isolated photosystem I preparations using time-resolved fluorescence analysis. *Biophys. J.* 53:733–745.
3. Holzwarth, A. R., W. Haehnel, R. Ratajczak, E. Bittersman, and G. H. Schatz. 1990. Energy transfer kinetics in photosystem I particles isolated from *Synechococcus sp.* and higher plants. *In* Current Research in Photosynthesis. Vol. II. M. Blatscheffsky, editor. Kluwer Academic Publishers, The Netherlands. 611–614.
4. Searle, G. F. W., R. Tamkivi, A. van Hoek, and J. T. Schaafsma. 1988. Temperature dependence of antenna chlorophyll fluorescence kinetics in photosystem I reaction center protein. *J. Chem. Soc. Farad. Trans. II.* 84:315–327.
5. Wittmershaus, B. P. 1987. Measurements and kinetic modelling of picosecond time-resolved fluorescence from photosystem I and chloroplasts. *In* Progress in Photosynthesis Research. Vol. 1. J. Biggins, editor. Martinus Nijhoff, The Hague. 75–82.
6. Mukerji, I., and K. Sauer. 1988. Temperature dependent steady state and picosecond kinetic fluorescence measurements of a photosystem I preparation from spinach. *In* Proc. C. S. French Symposium on Photosynthesis. Alan R. Liss Inc., New York. 105–122.
7. Owens, T. G., S. P. Webb, L. Mets, R. S. Alberte, and G. R. Fleming. 1989. Antenna structure and excitation dynamics in photosystem I. II. Studies with mutants of *Chlamydomonas reinhardtii* lacking photosystem II. *Biophys. J.* 56:95–106.
8. Maroc, J., J. Garnier, and D. Guyon. 1989. Chlorophyll-protein complexes related to photosystem I in *Chlamydomonas reinhardtii. J. Photochem. Photobiol. B: Biol.* 4:97–109.
9. Garnier, J., J. Maroc, and D. Guyon. 1986. Low temperature emission spectra and chlorophyll-protein complexes in mutants of *Chlamydomonas reinhardtii:* evidence for a new chlorophyll-*a*-protein complex related to photosystem. I. *Biochim. Biophys. Acta.* 851:395–406.
10. Shiozawa, J. A., R. S. Alberte, and J. P. Thornber. 1980. The P700-chl *a*-protein. Isolation and some characteristics of the complex in higher plants. *Arch. Biochem. Biophys.* 165:388–397.
11. Bengis, C., and N. Nelson. 1975. Purification and properties of the photosystem I reaction center from chloroplasts. *J. Biol. Chem.* 250:2783–2788.
12. Takahashi, Y., K. Hirota, and S. Katoh. 1985. Multiple forms of P700-chlorophyll a-protein complexes from *Synechococcus sp.:* the iron, quinone and carotenoid contents. *Photosynth. Res.* 6:183–192.
13. Golbeck, J. H., and J. M. Cornelius. 1986. Photosystem I charge separation in the absence of centers A and B. Optical characterization of the center "A2" and evidence for its association with the 64-kDa peptide. *Biochim. Biophys. Acta.* 849:16–24.
14. Golbeck, J. K. 1987. Structure, function and organization of the photosystem I reaction center complex. *Biochim. Biophys. Acta.* 895:167–204.
15. Golbeck, J. K., and D. A. Bryant, 1991. Photosystem I. *In* Current Topics in Bioenergetics. Vol. 16. C. P. Lee. editor. Academic Press, New York. 83–110.
16. Bengis, C., and N. Nelson, 1977. Subunit structure of the photosystem I reaction center. *J. Biol. Chem.* 252:4564–4569.
17. Okamura, M. Y., G. Feher, and N. Nelson. 1982. Reaction centers. *In* Photosynthesis. Vol. 1. Energy Conversion by Plants and Bacteria. Govindjee, editor. Academic Press, New York. 195–274.
18. Mullet, J. E., J. J. Burke, and C. J. Arntzen. 1980. Chlorophyll proteins of photosystem I. *Plant Physiol.* 65:814–822.
19. Wollman, F. A., and P. Bennoun. A new chlorophyll-protein complex related to photosystem in *Chlamydomonas reinhardtii. Biochim. Biophys. Acta.* 680:352–360.
20. Ish-Shalom, D., and I. Ohad. 1983. Organization of chlorophyll-

protein complexes of photosystem I in *Chlamydomonas reinhardtii. Biochim. Biophys. Acta.* 722:497–507.

21. Holzwarth, A. R. 1989. Application of ultrafast laser spectroscopy for the study of biological systems. *Quart. Rev. Biophys.* 22:239–326.
22. van Grondelle, R., and V. Sundström. 1988. Excitation energy transfer in photosynthesis. 1988. *In* Photosynthetic Light-Harvesting Systems. H. Scheer and S. Schneider, editors. Walter de Gruyter, New York. 403–438.
23. Pearlstein, R. M. 1982. Excition migration and trapping in photosynthesis. *Photochem. Photobiol.* 35:835–844.
24. Jean, J., C.-K. Chan, G. R. Fleming, and T. G. Owens. 1989. Excitation transport and trapping on spectrally disordered lattices. *Biophys. J.* 56:1203–1215.
25. Pullerits, T., and A. Freiberg. 1991. Picosecond fluorescence of simple photosynthetic membranes: evidence of spectral inhomogeneity and directed energy transfer. *Chem. Phys.* 149:409–418.
26. Lyle, P. A., and W. S. Struve. 1991. Temperature dependence of antenna excitation transport in native photosystem I particles. *J. Phys. Chem.* 95:4152–4158.
27. Gillie, J. K., G. J. Small, and J. H. Golbeck. 1989. Nonphotochemical hole burning of the native antenna complex of photosystem I (PSI-200). *J. Phys. Chem.* 93:1620–1627.
28. Mukerji, I., and K. Sauer. 1990. A spectroscopic study of a photosystem I antenna complex. *In* Current Research in Photosynthesis. Vol. II. M. Baltscheffsky, editor. Kluwer Academic Publishers, The Netherlands. 321–412.
29. van der Laan, H., Th. Schmidt, R. W. Visschers, K. J. Visscher, R. van Grondelle, and S. Völker. 1990. Energy transfer in the B800-850 antenna complex of the purple bacteria *Rhodobacter spheriodes:* a study by hole burning. *Chem. Phys. Letts.* 170:230–238.
30. Jia, Y., J. M. Jean, M. M. Werst, C.-K. Chan, and G. R. Fleming. 1992. Simulations of the temperature dependence of energy transfer in the PSI core antenna. *Biophys. J.* In press.
31. Friesner, R., M. Pettitt, and J. M. Jean. 1985. Calculations of temperature dependent multimode resonance Raman line shapes for harmonic potential surfaces. *J. Chem. Phys.* 82:2918–2926.
32. Harris, R. A., R. A. Mathies, and W. T. Pollard. 1986. Simple interpretation of dephasing in absorption and resonance Raman theory. *J. Chem. Phys.* 85:3744–3748.
33. Surzychi, S. 1971. Synchronously grown cultures of *Chlamydomonas reinhardtii. Methods Enzymol.* 23:67–73.
34. Peter, G. F., O. Mackold, and J. P. Thornber. 1988. Identification and isolation of photosystem I and photosystem II pigment proteins of higher plants. *In* Methods in Plant Biochemistry. L. J. Rogers, editor. Academic Press, New York.
35. Hayama, T., and B. Ke. 1972. Difference spectra and extinction coefficients of P700. *Biochim. Biophys. Acta.* 267:160–171.
36. Thornber, J. P. 1969. Comparison of the chlorophyll-protein complex isolated from a blue-green alga with chlorophyll-protein complexes obtained from the green bacteria and higher plants. *Biochim. Biophys. Acta.* 172:230–241.
37. Chang, M. C., S. H. Courtney, A. J. Cross, R. J. Gulotty, J. W. Petrich, and G. R. Fleming. 1985. Time-correlated single photon counting with microchannel plate detectors. *Anal. Instrum.* 14:433–464.
38. Gulotty, R. J., L. Mets, R. S. Alberte, and G. R. Fleming. 1985. Picosecond fluorescence study of photosynthetic mutants of *Chlamydomonas reinhardtii:* origin of the fluorescence decay of chloroplasts. *Photochem. Photobiol.* 41:487–496.
39. Brody, S. S., and E. Rabinowitch. 1957. Excitation lifetimes of photosynthetic pigments in vivo and in vitro. *Science (Wash., DC).* 125:555–561.
40. Butler, W. L., C. J. Tredwell, R. Malkin, and J. Barber. 1979. The relationship between the lifetime and yield of the 735 nm fluorescence of chloroplasts at low temperatures. *Biochim. Biophys. Acta.* 545:309–315.
41. Nechushtai, R., S. D. Nourizadeh, and J. P. Thornber. 1986. A reevaluation of the fluorescence of the core chlorophylls of photosystem I. *Biochim. Biophys. Acta.* 848:193–200.
42. Bassi, R., and D. Simpson. 1987. Chlorophyll-protein complexes of barley photosystem I. *Eur. J. Biochem.* 163:221–230.
43. Dunahay, T. G., and A. L. Staehelin. 1985. Isolation of photosystem I complexes from octyl glucoside/sodium dodecyl sulfate solubilized spinach thylakoids. *Plant Physiol.* 78:606–613.
44. Herrin, D. L., F. G. Plumley, M. Ikeuchi, A. S. Michaels, and G. W. Smith. 1987. Chlorophyll antenna proteins of photosystem I: topology, synthesis and regulation of the 20-kDa subunit of *Chlamydamonas* light-harvesting complex of photosystem I. *Arch. Biochem. Biophys.* 254:397–408.
45. Tapie, P., Y. Choquet, J. Breton, P. Delepelaire, and F.-A. Wollman. 1984. Orientation of photosystem-I pigments: investigation by low temperature linear dichroism and polarized fluorescence emission. *Biochim. Biophys. Acta.* 767:57–69.
46. Hunter, C. N., H. Bergström, R. van Grondelle, and V. Sundström. 1990. Energy transfer dynamics in three light-harvesting mutants of *Rhodobacter sphaeroides:* a picosecond spectroscopy study. *Biochemistry.* 29:3203–3207.
47. van Grondelle, R., H. Bergström, V. Sundström, R. J. van Dorssen, M. Vos, and C. N. Hunter. 1988. Excitation energy transfer in the light-harvesting antenna of photosynthetic purple bacteria: the role of the long-wavelength absorbing pigment B896. *In* Photosynthetic Light-Harvesting Systems. H. Scheer and S. Schneider, editors. Walter de Gruyter, New York. 519–530.